Received: 16 January 2021 | Accepted: 15 April 2021

DOI: 10.1002/vzj2.20133

Vadose Zone Journal

ORIGINAL RESEARCH ARTICLE

Root architecture development in stony soils

Shehan Morandage[1,2] | **Jan Vanderborght**[1] | **Mirjam Zörner**[1] | **Gaochao Cai**[3] | **Daniel Leitner**[4] | **Harry Vereecken**[1] | **Andrea Schnepf**[1]

[1] Forschungszentrum Jülich, Agrosphere (IBG-3), Jülich D-52428, Germany

[2] Institute of Soil Science and Land Evaluation, Biogeophysics, Univ. of Hohenheim, Stuttgart, Germany

[3] Chair of Soil Physics, Univ. of Bayreuth, Bayreuth D-95447, Germany

[4] Simulationswerkstatt, Leonding, Austria

Correspondence
Shehan Morandage, Forschungszentrum Jülich, Agrosphere (IBG-3), Jülich, Germany, D-52428.
Email: shehan.morandage@uni-hohenheim.de

Assigned to Associate Editor Thorsten Knappenberger.

Abstract

Soils with high stone content represent a challenge to root development, as each stone is an obstacle to root growth. A high stone content also affects soil properties such as temperature or water content, which in turn affects root growth. We investigated the effects of all soil properties combined on root development in the field using both experiments and modeling. Field experiments were carried out in rhizotron facilities during two consecutive growing seasons (wheat [*Triticum aestivum* L.] and maize [*Zea mays* L.]) in silty loam soils with high (>50%) and low (<4%) stone contents. We extended the CPlantBox root architecture model to explicitly consider the presence of stones and simulated root growth on the plot scale over the whole vegetation period. We found that a linear increase of stone content resulted in a linear decrease of rooting depth across all stone contents and developmental stages considered, whereas rooting depth was only sensitive to cracks below a certain crack density and at earlier growth stages. Moreover, the impact of precipitation-influenced soil strength had a relatively stronger impact on simulated root arrival curves during the vegetation periods than soil temperature. Resulting differences between stony and non-stony soil of otherwise the same crop and weather conditions show similar trends as the differences observed in the rhizotron facilities. The combined belowground effects resulted in differences in characteristic root system measures of up to 48%. In future work, comparison of absolute values will require including shoot effects—in particular, different carbon availabilities.

1 | INTRODUCTION

More than 10% stone content is found in 41% of Europe's soils (Stendahl et al., 2009), affecting both forested and agricultural areas (Cai, Vanderborght, et al., 2018; Hlaváčiková et al., 2018). Although stones are abundant in many areas and significantly affect vegetation dynamics, systematic investigation of stony soil physical and hydraulic properties has only recently been conducted (Hlaváčiková et al., 2018; Naseri et al., 2019). The effect of stones on root architecture development is even less well known (Cai, Vanderborght, et al., 2018) and has only been explicitly incorporated in few root architectural models (Jin et al., 2020; Schnepf et al., 2018). The combined effect of stones and corresponding soil properties on root architecture development at the plot scale has not yet been explicitly simulated.

Modeling approaches are often used along with field observations to investigate detailed root system architectures (RSAs) of plants and their interaction with the surrounding soil environment (Dunbabin et al., 2013; Postma et al., 2017;

Abbreviations: MR, minirhizotron; RAC, root arrival curve; RID, root intersection density; RLD, root length density; RSA, root system architecture; TDR, time domain reflectometry.

Schnepf et al., 2018). In order to identify parameters that characterize the RSA and how it develops as a function of the soil conditions and properties, experimental field sampling data have been combined with model simulations using an inverse modeling framework (Garré et al., 2012; Morandage et al., 2019; Pagès et al., 2012; Vansteenkiste et al., 2014; Ziegler et al., 2019). Stones have never been explicitly considered in those studies.

However, the presence of large stones affects rooting patterns of crops. When a root tip meets an obstacle that cannot be penetrated or pushed away by the root, the root tends to change its growth direction by bending away from the obstacle to find another path (Bizet et al., 2016; Fakih et al., 2017; Jin et al., 2020; Popova et al., 2013, 2016; Schnepf et al., 2018). Displacement of solid particles by roots depends on many factors such as soil depth, root diameter, solid diameter, length of root segment, and root type or plant type (Whiteley & Dexter, 1984). The ability of roots to grow through soils is a function of root diameter (dR) and grain diameter (dG). If the aspect ratio ($S = \mathrm{dR/dG}$) is small, the root apex cannot displace, deform, or penetrate the obstacle (Kolb et al., 2017) and the root changes its growth direction (Falik et al., 2005). These processes may lead roots to follow highly tortuous paths, and new lateral root emergence (Richter et al., 2009) that primarily affect the structure of the root system and rooting depth. The influence of stone content on soil properties and root system development are outlined in the paragraphs below.

Stony soils may have the same fine soil bulk density as non-stony soil; however, they differ in bulk soil porosity and thus bulk soil bulk density. Soil strength or soil penetration resistance is one of the most important factors (Kirby & Bengough, 2002) that determines roots' ability to overcome the soil resistance against root extension. Roots may exhibit different characteristics and alterations in their original morphology, depending on soil strength and compaction (Correa et al., 2019). It has been found that elongation rates of roots decrease with increasing soil strength (Bengough, 1997; Bengough et al., 2006; Houlbrooke et al., 1997; Taylor & Brar, 1991; Tracy et al., 2012), and that root length density (RLD) decreases with increasing penetration resistance (Pardo et al., 2000). Bulk density usually does not vary substantially with time; however, soil strength does due to the fluctuations of moisture content and soil matric potential. Soil penetration resistance increases also with decreasing water content and matric potential (Eavis, 1972; Jin et al., 2013). All of those properties are affected by stone content. Since roots grow around stones and explore only the fine materials around stones, roots may sense mainly the properties of fine materials. Stony soils may have the same fine soil bulk density as non-stony soil; however, they differ in bulk soil porosity and thus bulk soil bulk density.

Cracks are formed mostly in fine-grained soils due to changes in soil moisture dynamics and soil composition.

Core Ideas

- We present a dynamic root architecture model that considers macroscopic soil properties.
- Root elongation rate and preferred growth direction are influenced by stones.
- We simulate the effects of soil properties on root architecture development using field data.
- Only belowground effects are considered by the root architecture model.
- Similar trends in measured and simulated root growth are observed in two different soils.

Cracks in soils create weak passages, which allow roots to grow with minimum resistance while anchoring into the crack surfaces. These zones accumulate more water during rainfall or irrigation events and are more favorable for root functions during water stress periods than hard, less permeable zones (Grismer, 1992). In soils with high penetration resistance, cracks may be of importance to root system development, as they provide loose zones with minimal resistance through which roots can reach deeper depths (Tardieu, 1994).

Previous studies showed that temperature changes the RSA, affecting length, rooting depth, root elongation rates, branching intensity, surface area, growth direction, and lateral branch angles (Kaspar & Bland, 1992; Macduff et al., 1986; Nagel et al., 2009; Onderdonk & Ketcheson, 1973; Vincent & Gregory, 1989). Several studies were conducted to investigate the effect of temperature on root growth of different plants: cotton grass (*Eriophorum vaginatum* L.; Ellis & Kummerow, 1982; Tardieu, 1994), cotton (*Gossypium hirsutum* L.; McMichael & Quisenberry, 1993), alfalfa (*Medicago sativa* L.; Ellis & Kummerow, 1982), and oilseed rape (*Brassica napus* L.) and barley (*Hordeum vulgare* L.; Macduff et al., 1986). These studies indicated that certain crops have a specific optimum temperature of reaching the maximum growth rate. Increasing temperature does not always increase root elongation rates because after reaching the optimum temperature, root growth starts to decrease with increasing temperature (Drennan & Nobel, 1998; McMichael & Quisenberry, 1993). For instance, winter wheat (*Triticum aestivum* L.) shows root length increases with increasing temperature up to ~20 °C and starts to decrease thereafter (Huang et al., 1991). Furthermore, the optimum, minimum, and maximum temperatures for root development and elongation rates vary with genotypes as well as crop types (Sattelmacher et al., 1990).

Several root growth models were introduced to include soil physical, chemical, and climatic features such as biopores (Landl et al., 2017), soil strength (de Moraes et al., 2018;

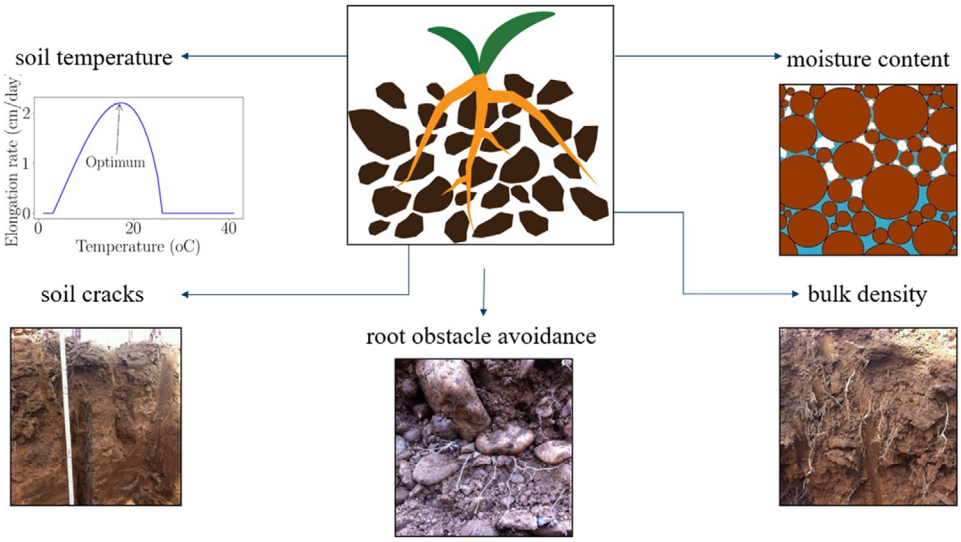

FIGURE 1 Main factors that influence the root growth dynamics of a plant

Grant, 1993), root obstacle avoidance (Fakih et al., 2017; Jin et al., 2020), temperature (Nagel et al., 2009), and moisture content (de Moraes et al., 2018). Furthermore, some studies were conducted to understand the effect of soil properties on root growth under field conditions based on root growth models (de Moraes et al., 2019; Landl et al., 2019). The main challenge in this regard is the lack of dynamic soil and field root sampling data and to include complex soil structures and dynamics in the models. Figure 1 illustrates prominent soil physical conditions that influence root growth dynamics and root architecture development based on plants' growth medium.

To study the effect of stone content on root growth in the field, two minirhizotron (MR) facilities were established in Selhausen, Germany. The two sites are 150 m apart from each other and can be considered to experience equal climatic conditions. They also have similar fine soil properties (silty loam) but differ substantially in their stone contents (60 and 4%, respectively). Throughout this manuscript, we use the terms "stony soil" and "cracked soil" to refer to the soils of these two sites. During the last 4 yr of root observations, significant differences in root mass, root depth distribution, and maximum rooting depth in two different sites were observed (Cai et al., 2016). The differences between sites are remarkably more significant than the differences between the years (growing periods) and crops. However, these observations and governing factors cannot be explained without proper representation of the underlying root growth mechanisms. Therefore, we used a root architecture model to examine the effect of stone content and corresponding differences in soil properties on root distribution at the two sites with the same climate and crops. We investigated whether the difference in stone content and related soil properties can explain the observed differences in root system development by numerical modeling.

2 | MATERIALS AND METHODS

2.1 | Field experiments

2.1.1 | The experimental site

We conducted field experiments at two rhizotron facilities in Selhausen, Germany (50°52′07.8″ N, 6°26′59.7″ E), which are located ~150 m apart from each other. As described in Cai, Vanderborght, et al. (2018), the main soil in the field is a Haplic Luvisol that developed in a layer with a silt loam texture (Weihermüller et al., 2007). The thickness of the silt loam layer varies strongly along the slope of the field. It is up to 3 m thick at the bottom of the slope and not present at the top. One rhizotron facility is located at the top (stony) and has a stone content of >60%. The second rhizotron facility (cracked) is located at the bottom of the slope. It has a silty loam soil with a negligible amount of stone content (<4%) that is also characterized with deep soil cracks.

Table 1 shows the particle size distribution of the soils of the two rhizotron facilities. Each facility covers an area of 68.25 m^2 (7 m wide and 9.75 m long) and is separated into three subplots with three different water treatments. The first plot was kept dry using a sheltering system, which sheltered out the rainwater. The middle plot was fed by rainwater. The third plot was irrigated to supply the necessary plant water demand. In this study, we used only the data collected from the rain-fed plot because this plot represents the natural climatic conditions of the area. Soil moisture content was measured hourly using time domain reflectometry (TDR) sensors (Campbell Scientific, Inc.). The TDR data were converted to water content based on the Topp equation for the cracked facility and a combination of the Topp equation and Complex Refractive Index Model (CRIM) model for the stony

TABLE 1 Volume fractions of soil and gravel at the Selhausen test site, modified after Weihermüller et al. (2007) and Stadler et al. (2015)

		Percentage			
		Stony facility		Cracked facility	
Name	Particle size	Depth < 30 cm	Depth > 30 cm	Depth < 30 cm	Depth > 30 cm
Gravel	mm	%			
Very coarse	>63	1.0	1.5[a]	2.4	1.2
Coarse	40–63	2.0	3.0[a]		
	20–40	3.0	4.6[a]		
Medium	10–20	5.0-	7.6[a]		
	6.3–10	7.0	10.7[a]		
Fine gravel	2.0–6.3	16.0	24.5[a]		
Stone fraction	>2.0	34	51.9	2.4	1.2
Fine fraction[b]	<2.0	33	23.1	57.6	58.8
Porosity	–	33	25	40	40

[a]Estimated based on the assumption that the distribution in the size classes is the same as in <30-cm depth, adjusted based on known total stone content.
[b]Distribution of fine fraction (<2.0 mm) of stony (sand = 36%, silt = 50%, and clay = 14%) and cracked facility (sand = 12%, silt = 68%, and clay = 18%).

facility. The MPS-2 sensors (Decagon Devices) measured the soil water potential along with the soil temperature for both facilities half-hourly. In addition to MPS-2 sensors, soil water potentials were measured by tensiometers (UMS) hourly (see Cai et al. [2016] for a detailed description of the installation setup and experimental procedure in the MR facilities in Selhausen). We measured crop height and leaf area index weekly during the entire growing seasons to study the aboveground shoot development differences in the two sites. Furthermore, climatic data were collected from the climate station next to the field site.

2.1.2 | Grain size analysis and soil classification

The grain size distribution was obtained from the soil analysis of the Selhausen test site (Cai et al., 2016; Stadler et al., 2015; Weihermüller et al., 2007) (Table 1). Facility 2 (cracked) consists of >96% of particles with diameters smaller than 2 mm. Therefore, it is unlikely to see an effect of stones on rooting patterns in the cracked facility. The detailed grain size analysis of fine fractions of both facilities is carried out by the previous studies (Cai et al., 2016). In order to determine the particle size distribution of stone fraction (>2 mm) in the stony facility, we collected a block (240 × 250 × 65 mm) of soil from the stony facility. The soil sample was dried, and stones (>2 mm) were separated from the fine soil fraction (<2 mm). The stone fraction was further separated based on the diameter classes of 2–6.3, 6.3–20, 20–63, and >63 mm.

2.1.3 | Experimental design and agricultural management

Winter wheat was sown on 26 Oct. 2015 and harvested on 22 July 2016. Maize (*Zea mays* L.) was sown on 3 May 2017 and harvested on 12 Sept. 2017. Winter wheat was sown at a population density of 450 plants m^{-2} with 3-cm distance between plants in a row and 12-cm distance between rows. A total number of 750 maize seeds were sown (~10 plants m^{-2}) in 10 rows with inter-row spacing of 75 cm and 13-cm spacing between two plants within a row.

2.1.4 | MR root observations

Root growth was observed through horizontally installed 7-m-long, 6.4-cm-o.d. transparent tubes using a Bartz MR camera system (VSI /Bartz Technology Corporation). Rhizotubes are installed at six different depths of 10, 20, 40, 60, 80, and 120 cm below the soil surface in each facility. There are three replicate tubes at each depth, accounting for 54 tubes in each facility. The camera captures 1.65-cm-long and 2.35-cm-wide real-size images (Cai, Morandage, et al., 2018). Images were taken at 20 fixed positions from the left- and right-hand sides of each tube weekly (or biweekly) during the growing seasons. We conducted 22 and 12 measurements for winter wheat and maize, separately, during the growing seasons. The images were processed using the root imaging software Rootfly (Zeng et al., 2008) to obtain the number of roots per image. To get

one-dimensional depth profiles representative for the plot, we computed the average root count per image over all 40 images taken at predefined positions along each 7-m-long horizontal tube. We then followed Option 2 of Cai et al. (2016) and computed the RLD by dividing the number of root counts by the product of image width and radius of the rhizotube. This is an estimation based on the assumption that roots would grow nearly vertically through the soil volume now occupied by the rhizotube. To know the absolute value of root length densities would require calibration with actual root length measurements, such as from coring. For many applications, only the normalized RLD distribution is needed (e.g., in computing the sink term for root water uptake from soil; Cai et al., 2016).

2.2 | Root growth simulations (the root architecture model CPlantBox)

The root architecture model of CPlantBox (Schnepf et al., 2018; Zhou et al., 2020) was used to simulate the three-dimensional root architectures of winter wheat and maize root systems for full vegetation periods (240 d for winter wheat and 120 d for maize). CPlantBox simulates root systems with predefined RSA parameters, and each parameter of the RSA model is described by mean and standard deviation values that assign stochasticity to simulated root systems. Root systems can be simulated with or without considering the soil and environmental factors that affect root growth and distributions. Each of these effects is implemented in CPlantBox such that the RSA parameters are rescaled, and root growth is subjected to changes in soil and environmental conditions of the growth medium and the locality.

2.3 | Model setups for winter wheat and maize

The winter wheat root systems were simulated using the parameters of Morandage et al. (2019) with a 9-d time interval between two successive basal roots. Morandage et al. (2019) assumed that the basal roots emerge at once along with primary roots for root system simulations. For the simulation of the maize RSAs, we used the RSA parameter set of Postma and Lynch (2011).

Due to the model stochasticity, we performed 100 simulations for each scenario without stones and 50 repetitions for scenarios, including stones due to long simulation times. Each simulated root system represented a plant within a field. For wheat and maize, planting density was given by 12- and 75-cm inter-row spacing and 3- and 13-cm distance between plants, respectively. From the resulting root architectures in the field, we computed RLD profiles for comparison against observed RLD profiles. Since the simulation of multiple root systems in a virtual plot requires a higher computational demand, we simulated only one root system in each simulation step and repeated the simulations. The RLD was calculated by averaging over the representative area covered by a root system based on row and inter-row distances:

$$\mathrm{RLD}\ \left(\mathrm{cm\ cm^{-3}}\right) = \frac{\text{total root length of a horizontal slice}\ \left(\mathrm{cm\ cm^{-3}}\right)}{\text{inter row distance}\ (\mathrm{cm}) \times \text{inter plant distance}\ (\mathrm{cm})} \quad (1)$$

We considered different scenarios. First, we simulated the effects of each soil property on root system development separately, and finally, we compared their combined effect on simulated and real field sampling data.

2.4 | Modeling the influence of static soil physical properties on simulated root growth patterns

In this section, we describe how CPlantBox simulates the effect of prominent structural features (e.g., stones, soil bulk density, and cracks) on RLD distributions and rooting depths.

2.4.1 | Stone content and root obstacle avoidance

The model CPlantBox uses signed distance functions to simulate root growth in confined geometries (Schnepf et al., 2018). The signed distance function determines the distance of a given point (x) to the nearest boundary of the object. If the value is positive, x is inside Ω (inside the boundary); if it is negative, x is outside the boundary, and zero indicates that x is positioned on the boundary (Osher & Fedkiw, 2003):

$$f(x) = \begin{cases} \mathrm{d}(x, \partial\Omega), & x \epsilon \Omega^{+} \\ -\mathrm{d}(x, \partial\Omega), & x \epsilon \Omega^{-} \end{cases} \quad (2)$$

Using such signed distance functions to represent the geometry of stones explicitly, root tip heading during growth is changed repeatedly until the new position of the root tip is outside of any stones (Figure 2). The algorithm checks for each new root tip position, whether it lies outside any stones. If it does not, a new pair of axial and radial angles (α, β) is chosen as follows. First, only β is set to be uniformly random between $-\pi$ and π, whereas α is left unchanged. If, after a maximal number of trials, no new valid pair α and β has been found, α is increased by a small increment, and the procedure for finding an angle β starts again. This simple approach leads to a realistic root behavior at the boundaries, where thigmotropism can be observed (Schnepf et al., 2018). Because of

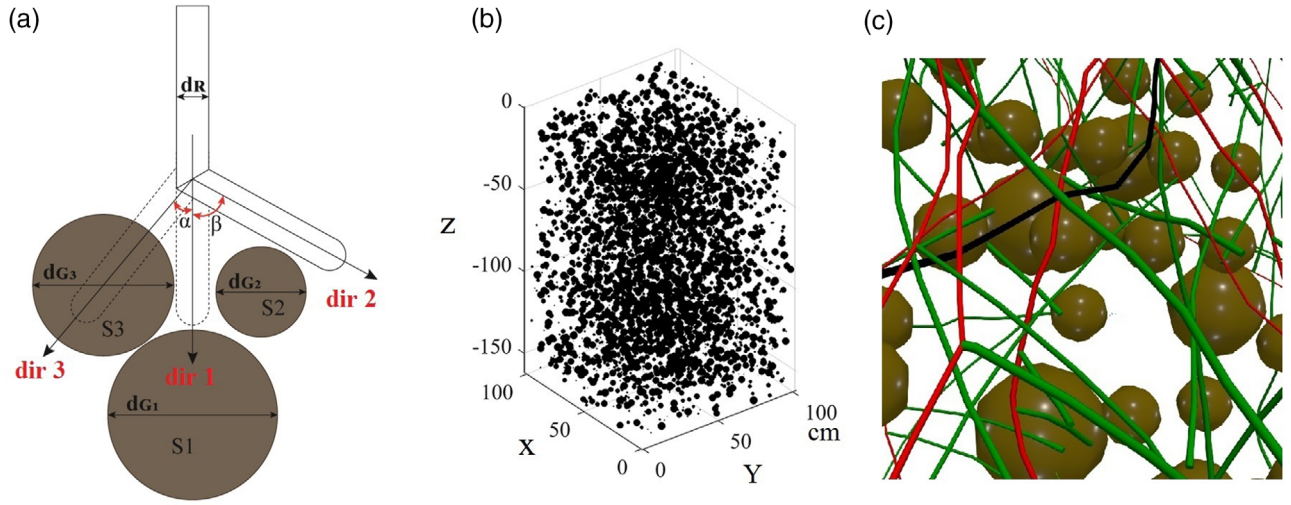

FIGURE 2 Deflection of root segments due to obstacle avoidance. (a) The axial and radial angles (α, β) are changed repeatedly until a new, obstacle-free growth direction is found. (b) Packing stones in a 100-cm × 100-cm × 160-cm soil block with different diameter classes to simulate root growth in stony soil, based on the compositions given in Table 1. (c) Root growth simulations with the influence of stones as obstacles (dR: root diameter; dG: grain diameter; S: stone obstacle; dir: growth direction; X, Y, Z: coordinate axes)

TABLE 2 Simplified distribution of particle sizes and respective percentages of the stony soil facility used for simulations

Total stone volume (>5 mm)	Distribution of stones in diameter classes, mm				
	5	10	20	40	80
	%				
Topsoil (19%)	8.0	5.0	3.0	2.0	1.0
Subsoil (28.9%)	12.2	7.6	4.6	3.0	1.5

TABLE 3 Root elongation rates of winter wheat (Colombi et al., 2017) and maize (Popova et al., 2016) observed in soils with different bulk densities

Parameter	Bulk density, g cm^{-3}				
	1.3	1.4	1.5	1.6	1.7
Elongation rate, wheat, cm d^{-1}	2.28	1.67	1.18	0.80	0.40[a]
Elongation rate, maize, cm d^{-1}	3.50	2.86	2.25	1.63	1.00

[a]Extrapolated value.

numerous deviations due to impenetrable obstacles, the final root length distribution may substantially change compared with roots grown in fine-grained soils.

Based on the grain size analysis of the stony soil of the stony facility, we categorized grain size distribution as percentages of spheres with 80-, 40-, 20-, 10-, and 5-mm diameter (Table 2). We assumed that stones with a diameter smaller than 5 mm can be considered as movable obstacles by roots and do not affect the growth direction of root trajectories. In contrast, stones larger than 5 mm cannot be moved by roots and therefore present an obstacle (Figure 2a). We further assume that the soil matrix of surrounding stones is homogeneous. In CPlantBox, we randomly selected stone positions and diameter classes to place all particles inside the selected soil domain with a size of 100 × 100 × 160 cm.

To study the dependence of root growth as a function of stone content, we selected five scenarios with decreasing packing densities to evaluate how increasing stone content affects rooting depths. The highest packing density was selected according to the composition of the stony soil given in Table 2, and the remaining four scenarios were chosen as 80, 60, 40, and 20% densities of the stone fractions of the stony facility. We repeated each scenario 50 times to compute the mean vertical root distributions with 1-cm depth intervals. Finally, we evaluated the changes in rooting depth as a function of increasing packing density for both wheat and maize crops.

2.4.2 | Root system response to different bulk densities

We simulated five scenarios with increasing soil bulk densities of 1.3, 1.4, 1.5, 1.6, and 1.7 g cm^{-3}. We obtained root elongation rates at different bulk densities based on laboratory studies published by Colombi et al. (2017) for wheat and Popova et al. (2016) for maize (Table 3) and rescaled the elongation rates accordingly. It should be noted that the elongation rates of these parameters were derived based on the early stages of the plants, and we assumed that the other root architecture parameters are not considerably influenced.

Finally, the root systems of winter wheat and maize crops were simulated 100 times for each scenario to compute the mean maximum rooting depth (D99) by taking the depth above which 99% of the total root length was observed.

2.4.3 | Role of soil cracks on rooting depth

The influence of cracks on root growth of winter wheat and maize crops was simulated using the approach of Landl et al. (2017) that considers cracks or macropores as anisotropies to the preferred root growth direction. In addition to changed root orientation due to cracks, the root elongation rate is also increased when roots grow inside the cracks due to decreased bulk densities. Since we did not have measured growth rates of roots inside cracks, we used the literature-derived root elongation rates of loose soil with a bulk density of 1 g cm^{-3}. Compared with the root elongation rate in field soil (1.55 g cm^{-3}), the elongation rate in the loosely packed soil inside the macropores (1 g cm^{-3}) was 200% larger (Valentine et al., 2012). To test the effect of crack intensities, we defined a 100-cm × 100-cm × 160-cm homogeneous soil domain and set the seed in the center of the soil domain at 3-cm depth. With this setup, we tested five scenarios with 5-mm-wide uniform cracks representing increasing crack intensities of 2, 5, 10, 20, and 50 cracks per 1-m length of the soil domain.

2.5 | Influence of dynamic soil conditions on root growth patterns

2.5.1 Soil temperature

To adapt growth rates according to measured soil temperatures, we rescaled the optimum elongation rates with a temperature-dependent impedance factor. The impedance factor was calculated using measured data half-hourly at six different soil depths (10, 20, 30, 60, 80, and 120 cm) (Supplemental Figures S1 [wheat] and S4 [maize]). The field-derived temperature values were obtained from 2015 November to 2016 July for winter wheat, and from 2017 May to 2017 September for maize. The relative root elongation rates were assigned to the CPlantBox model as grid-based values. When roots arrive at a certain depth, elongation rates are rescaled based on the temperature of that depth at the given time, according to Clausnitzer and Hopmans (1994):

$$\mathrm{VT}_{\mathrm{eff}} = \sin\pi(T)^{\sigma} \tag{3}$$

conditions where

1. $\mathrm{tem} > \mathrm{tem}_{\max}$ or $\mathrm{tem} < \mathrm{tem}_{\min} \mathrm{VT}_{\mathrm{eff}} = 0$

2. $T_{\mathrm{opt}} < 0.5(\mathrm{tem}_{\min} + \mathrm{tem}_{\max})$,
$$T = \frac{\mathrm{tem} - \mathrm{tem}_{\min}}{\mathrm{tem}_{\max} - \mathrm{tem}_{\min}},$$
$$\sigma = \frac{\log(0.5)}{\log\left(\frac{T_{\mathrm{opt}} - \mathrm{tem}_{\min}}{\mathrm{tem}_{\max} - \mathrm{tem}_{\min}}\right)}$$

3. $T_{\mathrm{opt}} > 0.5(\mathrm{tem}_{\min} + \mathrm{tem}_{\max})$,
$$T = \frac{\mathrm{tem} - \mathrm{tem}_{\max}}{\mathrm{tem}_{\min} - \mathrm{tem}_{\max}},$$
$$\sigma = \frac{\log(0.5)}{\log\left(\frac{T_{\mathrm{opt}} - \mathrm{tem}_{\max}}{\mathrm{tem}_{\min} - \mathrm{tem}_{\max}}\right)}$$

where tem is the measured soil temperature (˚C), T_{opt} is the genotype-specific optimal temperature for root growth, and $\mathrm{tem}_{\max}$ is the maximum and $\mathrm{tem}_{\min}$ is the minimum temperature within which root elongation occurs. Maximum, minimum, and optimum temperatures for winter wheat were set to 25, 2, and 16.3 ˚C, respectively (Porter & Gawith, 1999), and for maize were set to 40.1, 12.6, and 26.3 ˚C (Sánchez et al., 2014). We simulated the root systems, root development, and root arrival curves (RACs) under the optimal conditions and according to the temperature dynamics of the stony facility and the cracked facility.

2.5.1 | Effect of penetration resistance and matric potential on root growth

We computed root elongation rates as functions of bulk density measurements, and water content, and matric potential observations in 30-min time intervals at six different depths in two field sites. According to Dexter (1987), the relative root elongation $\mathrm{VR}_{\mathrm{eff}}$ can be expressed as

$$\mathrm{VR}_{\mathrm{eff}} = \frac{R}{R_{\max}} = \left[\frac{-\psi_0}{\psi_w} + \exp^{-0.6931\left(P_R/P_{R1/2}\right)}\right] \tag{4}$$

where $R_{\max}$ is the maximum rate of root elongation (cm d^{-1}), R is the root elongation rate (cm d^{-1}), ψ_0 is the matric potential (kPa), which was measured in field sites (Supplemental Figures S3 [wheat] and S6 [maize]), ψ_w is the matric potential at the wilting point (−1,500 kPa), P_R is the penetrometer resistance (MPa), and $P_{R1/2}$ is the penetration resistance value at which the root elongation rate decreases to half of its maximum value. The $P_{R1/2}$ values were obtained from the published data of wheat (Colombi et al., 2017) and maize (Bengough et al., 2011). The penetration resistance dynamics, P_R can be adjusted at each time step based on normalized

moisture content (sp) and normalized bulk density (ρ_b) (Vaz et al., 2013).

$$PR = \exp^{(1.5 + 2.18 \times \rho_b - 4sp)} \quad (5)$$

where

$$sp = \frac{\theta_v - \theta_p}{\theta_s - \theta_p}$$

and

$$\rho_b = \frac{\rho_b - \rho_{bmin}}{\rho_{bmax} - \rho_{bmin}}$$

where θ_v is the volumetric water content ($cm^3\ cm^{-3}$), θ_s is the saturation (= porosity), θ_p is the permanent wilting point ($cm^3\ cm^{-3}$), ρ_b is the measured bulk density ($g\ cm^{-3}$), ρ_{bmin} is the minimum soil bulk density ($g\ cm^{-3}$), and ρ_{bmax} is the maximum soil bulk density ($g\ cm^{-3}$).

Although the sensors measure the soil hydraulic properties of the bulk soil (stones + fine soil), roots experience mostly the influence of fine materials of soil, as roots do not explore the stone fraction of the soil. Therefore, soil hydraulic properties that determine the root–soil penetration resistance in the fine soil fraction should be considered, and the bulk volumetric water content data should be converted into fine soil values in the stony soil site (Naseri et al., 2019). According to Hlaváčiková et al. (2018), the bulk volumetric water content θ^b is defined as

$$\theta^b = \left(1 - R_v\right)\ \theta^f + R_v\theta^{rf} \quad (6)$$

where R_v is the stoniness ($cm^3\ cm^{-3}$), and θ^{rf} is the volumetric water content of stones ($cm^3\ cm^{-3}$), and θ^f is the volumetric water content of fine soil ($cm^3\ cm^{-3}$). If we assume that the $\theta^{rf} = 0$, fine soil water content, θ^f can be computed as $\theta^f = \theta^b/(1 - R_v)$. The fine soil porosity and wilting point of the topsoil were thus computed to be 0.5 and 0.15, and the same parameters of subsoil were 0.52 and 0.13, respectively. We used measured porosity (0.4) and wilting point (0.19) for the loamy soil in the cracked facility (Cai et al., 2016). We selected the average, maximum, and minimum bulk density of 1.3 , 1.7, and 1.1 $g\ cm^{-3}$ for the stony soil facility, and 1.5, 1.7, 1.3 $g\ cm^{-3}$ for the cracked soil facility, respectively. Based on the above settings, the elongation rates of each root tip at each time step and depth were derived using measured water content (Supplemental Figures S2 [wheat] and S5 [maize]), and water potential (Supplemental Figures S3 [wheat] and S6 [maize]). Then, we simulated wheat and maize root systems using the rescaled growth rates due to fluctuations of moisture contents to compute the dynamics of RLD throughout the growing season, taking observations at 10-, 20-, 40-, 60-, 80-, 120-cm depths.

TABLE 4 The effect of individual factors used to compute the combined effective elongation rates of two rhizotron facilities and simulate the root growth based on measured soil properties and macroscopic features

Soil type	Temperature	Penetration resistant	Macroscopic features	
			Cracks	Stones
1. Stony facility	Yes	Yes	No	Yes
2. Cracked facility	Yes	Yes	Yes	No

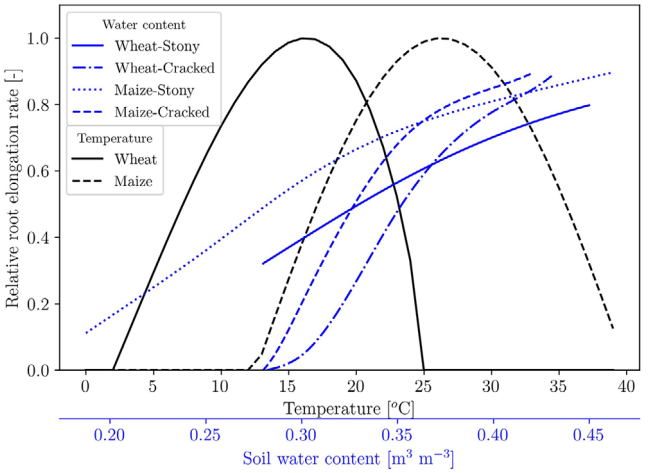

FIGURE 3 The relationship between relative root elongation rates of wheat and maize and the properties of growth medium: soil temperature (Clausnitzer & Hopmans, 1994), soil water potential, and soil moisture content (Dexter, 1987 ; Bengough et al., 1997 ; Dexter & Hewitt, 1978) of stony and cracked facilities

2.6 | Combining all effects based on field data to simulate root development in the two field sites

Finally, we combined all the individual effects, including temperature, water content, water potential, soil bulk densities, and respective penetration resistance on root development, in simulations and calculating the final RLD distributions of wheat and maize in both rhizotron facilities. Both facilities were exposed to the same climatic conditions, and the same crops were grown. The key difference is the stone content (stony facility) and the presence of cracks due to desiccation (cracked facility). The impedance to single root elongation as affected by individual physical properties is shown in Table 4 and Figure 3 for wheat and maize. The adjusted site-specific elongation rates were multiplied to calculate the combined effective elongation rates, V_{eff}.

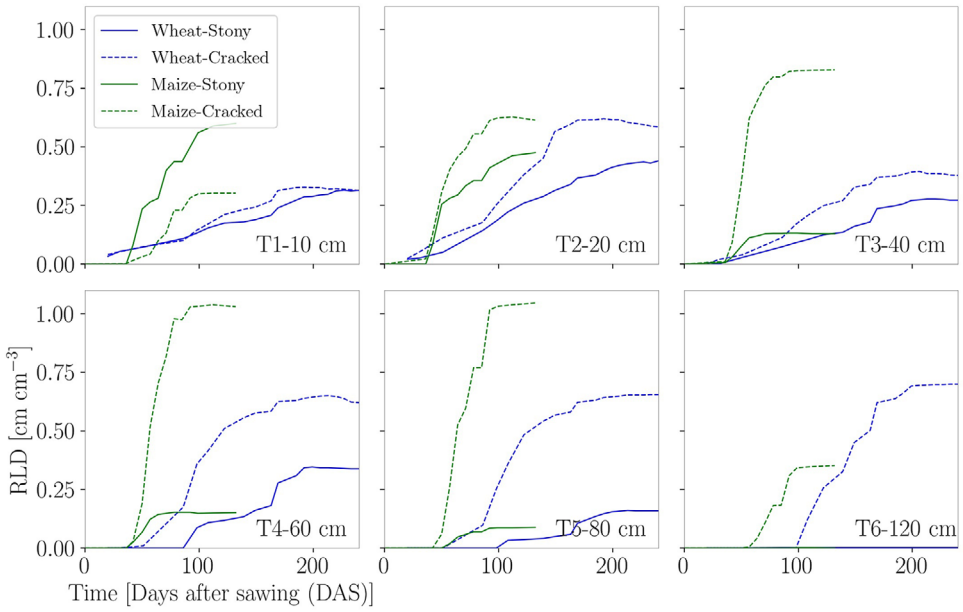

FIGURE 4 Root arrival curves observed in rhizotubes located at 10-, 20-, 40-, 60-, 80-, and 120-cm depths during the growing seasons of wheat and maize in both rhizotron facilities. RLD, root length density

$$V_{\text{eff}} = \text{VT}_{\text{eff}} \times \text{VR}_{\text{eff}} \times V_{\text{m}} \quad (7)$$

where VT_{eff} was temperature-induced root elongation rate, VR_{eff} was relative elongation due to penetration resistance, and V_{m} is the effects of macroscopic features (stones and cracks).

3 | RESULTS AND DISCUSSION

3.1 | Measured RACs and RLD profiles of winter wheat and maize in stony and cracked soils

Our MR data are useful for investigating the development of root systems at different depths during the entire duration of the vegetation period. Figure 4 shows the RACs, measured at 10-, 20-, 40-, 60-, 80-, and 120-cm soil depths of winter wheat and maize obtained during the 2015–2016 and 2017 growing seasons, respectively. In both experimental facilities, winter wheat reached its maximum root development ~200 d after sowing and maize roots 100 d after sowing. In the cracked soil, wheat roots arrived at 120-cm depth after 120 d, whereas there were hardly any roots observed at this depth in the stony soil.

In soil either with or without stones or cracks, winter wheat roots reached up to 40-cm depths within the first month. After the first month, root development in the silty loam (cracked) soil was faster than in the stony soil. The first arrivals of wheat roots were observed at 60- and 80-cm depth after 51 and 86 d in the silty loam (cracked) soil. If stones were present, wheat roots had reached 60- and 80-cm depths after 86 and 98 d. In the cracked soil, wheat roots arrived at 120-cm depth after 120 d, whereas there were hardly any roots observed at this depth in the stony soil.

Regardless of the soil type, maize roots reached the first 40 cm in within the first month and 60 cm in 38 d after sowing. The arrivals of maize roots at 80-cm depth in stony and cracked soil were observed 53 and 46 d, respectively, after sowing. We observed roots at 120-cm depth in the cracked soil by 53 d, whereas no roots were observed at the same depth in the stony soil. Additional excavation data confirmed the tortuous path around the stones in the stony soil and that maximum rooting depth did not exceed 100 cm (Supplemental Figure S8). Quite contrary, deep excavation in the cracked facility revealed a maximum rooting depth of 170 cm for maize (i.e., roots grow well below our deepest observation point at 120-cm depth).

The MR data are also presented as RLD profiles at the end of the vegetation period in Figure 5, together with the simulated and literature-derived range of RLD profiles for the two crops. We can see that the absolute values of observed root length densities do not compare with the simulated ones and also fall outside of the literature range of RLD profiles, except for maize in the stony facility. This can be expected due to our conversion method from root counts to RLD. However, the shapes also do not match well with the simulated and literature-derived range. Interestingly, the rather unusual convex shape of maize in the cracked facility was corroborated by the root intersection density (RID) data obtained from trenches in the year 2017 (Supplemental Figure S7). Furthermore, the MR data show small root length densities in the

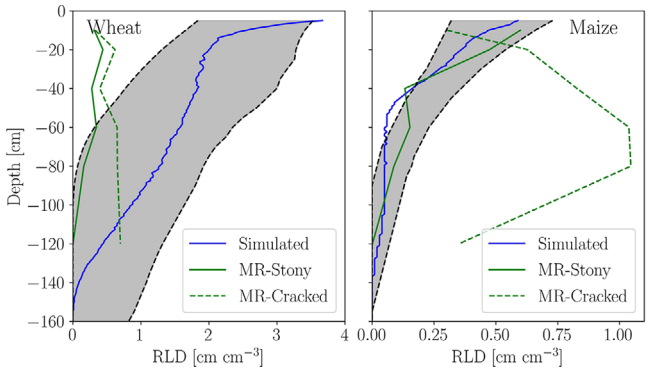

FIGURE 5 Root length density (RLD) distribution of winter wheat and maize at the end of the growing seasons measured by the minirhizotron (MR) method (green) plotted against the simulated RLD curves (blue) without considering the influence of soil and environmental factors and using standard winter wheat and maize input parameter sets of CPlantBox. The solid green lines indicate the measurements from the stony facility, and the dashed green lines indicate the cracked facility MR measurements. The gray shaded areas indicate root length density profiles derived based on measured data from the literature of wheat (Palta et al., 2004; Wasson et al., 2014; White et al., 2015; Xu et al., 2016; Zhang et al., 2009) and maize (Buczko et al., 2008; Gao et al., 2010; Mekonnen et al., 1997; Postma & Lynch, 2012; Zhan & Lynch, 2015; Zhuang et al., 2001)

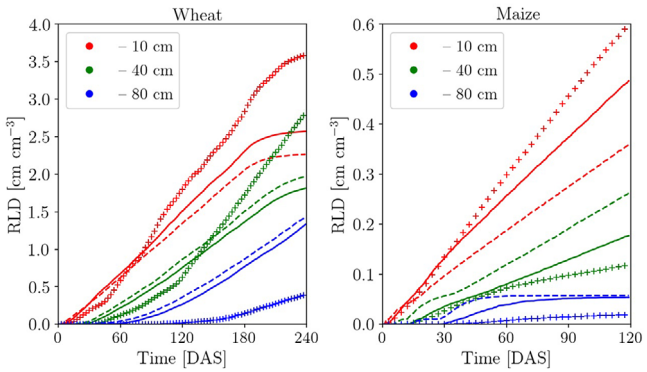

FIGURE 6 Simulated root arrival curves at different depths of wheat (left) and maize (right) in homogeneous soil (solid line) and soils with only the influence of cracks of silty loam soil (cracked facility, dashed line), and in stony soil (stony facility, + markers). DAS, days after sowing

top 40 cm. This is in line with other MR observations that are often known to underestimate RLD in the top 30–40 cm (Hulugalle et al., 2015; Postic et al., 2019; Svane et al., 2019) due to influence of the tubes that may alter root development, lack of contact between soil and tubes, and the position of the tubes relative to the seed positions (Ephrath et al., 1999). Preferential growth along is likely to be less important in the Selhausen rhizotron facilities because of the horizontally installed tubes.

Our main goal was therefore to compare the relative, not absolute, differences of characteristic root system measures between stony and cracked soils as observed and simulated. In the Section 3.2, we present the simulation results of the simulated root length densities using the input parameters from CPlantBox as described in Section 2.3 and demonstrate how they are affected (a) by each of the measured soil properties individually and (b) by all properties combined. For this, we informed the model with the measured values of soil temperature, soil water content, matric potential at 10-, 20-, 40-, 60-, 80-, and 120-cm depth, monitored during the whole vegetation period (data are available in the supplemental material).

3.2 | Simulated RLD distributions of winter wheat and maize before explicit consideration of the soil properties

Literature data of RLDs of wheat and maize are highly variable. Some studies show RLD values as high as 60 cm cm^{-3} and as slow as 0.5 cm cm^{-3} for mature root systems of wheat (Ephrath et al., 1999; Mekonnen et al., 1997; Svane et al., 2019; Zuo et al., 2006). However, most of the literature data indicate similar characteristics in the shape of the RLD curve (i.e., a shape that shows higher RLD in the topsoil and then decreasing with depth). The gray shaded area in Figure 5 is the envelope of available published RLD profiles (extreme RLD values that are indicated in published data were excluded), encompassing many different environmental conditions and thus representing a range of plausible RLD values. The root length densities obtained from CPlantBox model simulations fit well within that range of literature data for both crops.

3.3 | Influence of stones and cracks on root growth dynamics

Figure 6 shows the influence of stones and cracks on the simulated root growth of winter wheat and maize. Cracks stimulate the development of roots in the deeper depths (see Figure 6, blue dashed line), whereas stones prevent roots from penetrating deeper into the soil profile in comparison with the simulations of homogeneous soil. Therefore, a higher RLD is found in the upper layers (see Figure 6, red makers). The simulated maximum rooting depths at the end of the growth period were 130, 88, 135 cm for wheat and 123, 81, 134 cm for maize in homogeneous soil, stony soil, and soil with cracks, respectively.

3.4 | Sensitivity analysis of static soil properties on maximum rooting depth

The effect of stone content, crack intensity, and bulk density of soil on maximum rooting depth is summarized in Figure 7 for

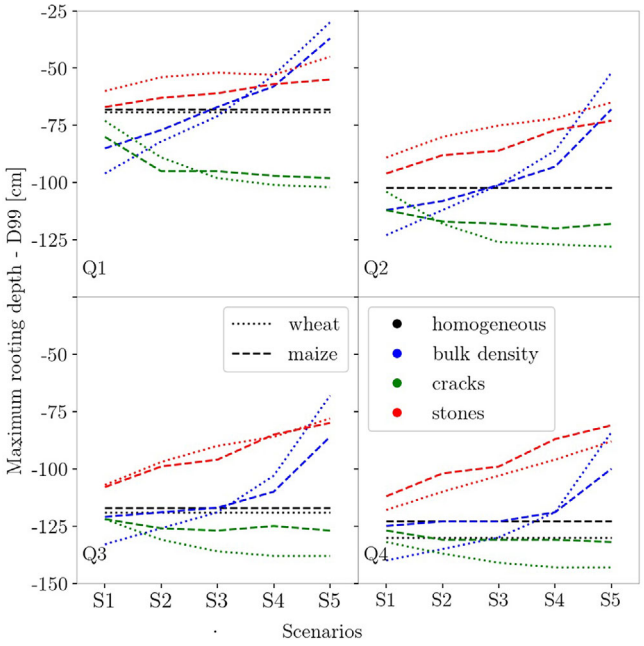

FIGURE 7 Sensitivity of the maximum rooting depths (D99 = depth above which 99% of root lengths observed) of wheat (dotted lines) and maize (dashed lines) on bulk density (blue lines), crack intensity (green lines), and stone content (red lines) in comparison with root growth patterns in homogeneous soil (black lines). Subplots Q1, Q2, Q3, and Q4 correspond to each quartile of the entire growth period of each crop type. S1, S2, S3, S4, and S5 represent the systematic increase of bulk densities (1.3, 1.4, 1.5, 1.6, and 1.7 g cm^{-3}), crack intensities (2, 5, 10, 20, 50 m^{-1} of the cracked facility) and stoniness (20, 40, 60, 80, and 100% of the stony facility) of soil, respectively

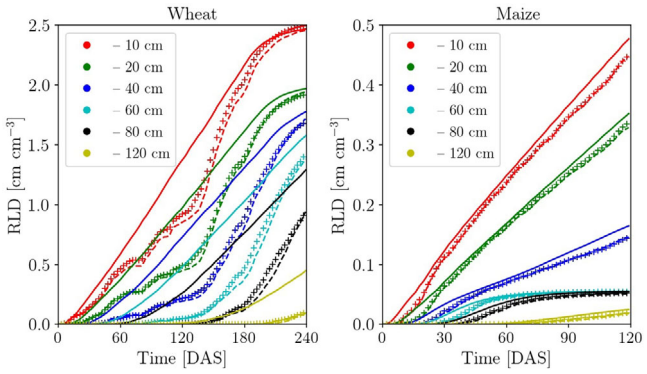

FIGURE 8 Simulated mean root arrival curves for winter wheat during the 2015–2016 growing season (left) for maize during the 2017 growing season (right) considering only the influence of temperature on root growth in the stony facility (+ markers) and the cracked facility (dashed line), plotted against the optimal temperature conditions (solid line) at depths of 10, 20, 40, 60, 80, and 120 cm. RLD, root length density; DAS, days after sowing

different stages during the vegetation period. The stone content and the size of the stones have a considerable influence on the maximum rooting depth of both wheat and maize crops. The effect of stones is more prominent in the later stages of the growth period as the difference between simulated rooting depths of homogenous soil and stony soil increase over time (differences in Q4 are higher than the differences in Q1). A linear decrease in rooting depths was observed due to a linear increase in stone content in the soil (see Figure 7, red lines). The maximum rooting depth increases with increasing density of cracks for both crops, indicating a −30-cm difference in the first 60 d of wheat and 30 d of maize, respectively. However, the sensitivity of rooting depth on cracks decreases with crop maturation, and for any age, roots are not sensitive to crack intensities that are higher than 10 m^{-1} for both crops (see Figure 7, green lines). The blue lines in Figure 7 show the effect of increasing bulk density on the maximum rooting depth. Root growth in relatively loose soil results in higher maximal rooting depth in early growth stages than the soil at 1.5 g cm^{-3} bulk density. For maize, this is leveled out at later growth stages at our parameterization, but not for wheat. Compacted soils, on the other hand, show a reduced maximum rooting depth at all growth stages.

3.5 | Effect of soil temperature on root growth and development

The measured soil temperature of the Stony soil facility is approximately 2 ˚C higher than the cracked facility (Supplemental Figure S1 [wheat] and S4 [maize]). The temperature differences cause slightly faster root growth in the stony soil (Figure 8). Winter wheat underwent temperatures ranging from 0 ˚C during the winter to 30 ˚C in the spring and maize experienced temperatures from 5 to 35 ˚C during the growth period. Notably, colder temperatures between February and March caused a reduction in elongation rates (in some cases, stopped the root elongation due to near-zero temperatures).

For wheat, the temperatures are far from optimal in both facilities. In the top layers, root development was delayed and reached the same RLD as the optimal temperature later. At the deepest depth (120 cm), root growth is reduced and does not catch up at later times. There is also a small difference in root length densities caused by the temperature difference between the two facilities. Compared with wheat, the temperatures are not as far from optimal for maize in both facilities. However, less than optimal temperatures hit the maize in the early phase, just after germination.

After stress periods, simulated growth curves show a steep growth compared to root growth under optimal conditions (Figures 8–9). The fact that impeded curves are sometimes even steeper than the steepest part of the optimum curve can be explained by the fact that both wheat and maize have fibrous root systems. In our model, basal roots emerge in specified time intervals near the root collar. If unimpeded, they could grow one after the other through the first 10-cm depth layer and further downwards. If impeded, it could happen that more and more basal roots emerge but cannot grow

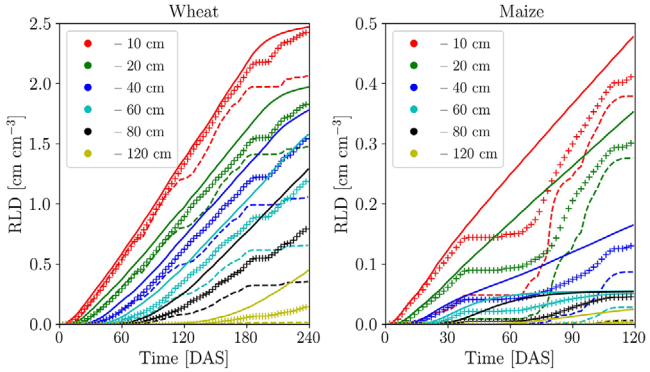

FIGURE 9 Simulated mean root arrival curves for winter wheat during the 2015–2016 growing season (left) and 2017 maize growing season (right) considering only the influence of soil strengths in the fine material of the stony facility (+ markers) and the cracked facility (dashed line), plotted against the optimal soil conditions (solid line) at depths of 10, 20, 40, 60, 80, and 120 cm. RLD, root length density; DAS, days after sowing

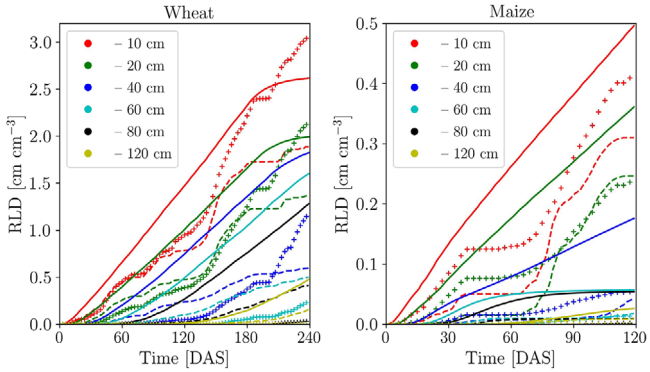

FIGURE 10 Comparison between simulated root arrival curves of optimal conditions (solid line) and root arrival curves of the stony facility (+ markers) the cracked facility (dashed line) for winter wheat during the 2015–2016 growing season (left) and 2017 maize growing season (right) considering the impact of all soil physical properties. RLD, root length density; DAS, days after sowing

past a certain soil depth before the next basal root arrives, thus increasing root tip density and the slope of the RAC.

3.6 | Effect of soil strength on root growth and development

Although the cracked facility soil has a higher water holding capacity (Supplemental Figures S2 and S5) and measured water content in stony soil is lower, the fine fraction of stony soil has a higher moisture content. Moreover, the wilting point of the cracked soil is higher than in the stony soil. Therefore, the anticipated lower penetration resistance and higher root growth rates due to apparent higher moisture contents in the cracked soil cannot be observed in simulated root growth patterns. The simulated RACs show that the fine soil matrix in the stony soil acts as a less resistant medium for root extension. Simulated root development in stony facility and cracked facilities is highly affected by penetration resistance (solid lines in Figure 9). Temporal variation of dry and wet weather conditions caused higher penetration resistance and stopped root growth in periods when the moisture content reached below the wilting point. In particular, dry summer conditions profoundly impeded root growth of maize.

3.7 | Effect of all factors combined on root growth and development

From Figure 6–9, we can see that stone content, temperature, and penetration resistance can have a substantial influence on RLD and root development. Although the influence of stone content was less important in the initial growing stage, it strongly affects final RLD and rooting depth with up to 60% difference compared with optimum root growth. The temperature was near to optimal for maize, whereas wheat experienced a substantial reduction of root growth between 80 and 120 d after sowing, with RLD <60% compared with optimal. However, root development could catch up with optimal growth by the end of the growing season except at 120-cm depth. Impedance due to penetration resistance resulted in permanently reduced root growth, even though the maize root system could recover after a drought period between 40 and 60 d after sowing, in which crops in the cracked facility suffered more than those in the stony facility.

Figure 10 now shows the simulated RAC data (winter wheat during the 2015–2016 growing season and maize in 2017) when considering all measured soil information simultaneously. As a comparison of absolute RLD values between simulations and observations is challenging, we compared relative differences between several observed and simulated characteristic root system measures in both facilities. Due to MR underestimation, we did not consider the RLD values in the top 40 cm. Figure 11 presents observed and modeled differences between stony and cracked soils, expressed as the difference of a root system measure between cracked and stony facilities relative to the cracked facility (silty loam soil) value. A bar towards the positive side means that the respective root system measure is larger in the cracked facility than in the stony facility. Likewise, a bar towards the negative side means that the respective root system measure is larger in the stony facility than in the cracked facility. Modeled and observed differences for both crops show that the loamy soil has a larger RLD below 40-cm depth than the stony soil. At any given depth, roots need longer to develop 50% of the RLD in the stony facility than in the cracked facility: both observations and simulations agree on this trend for wheat.

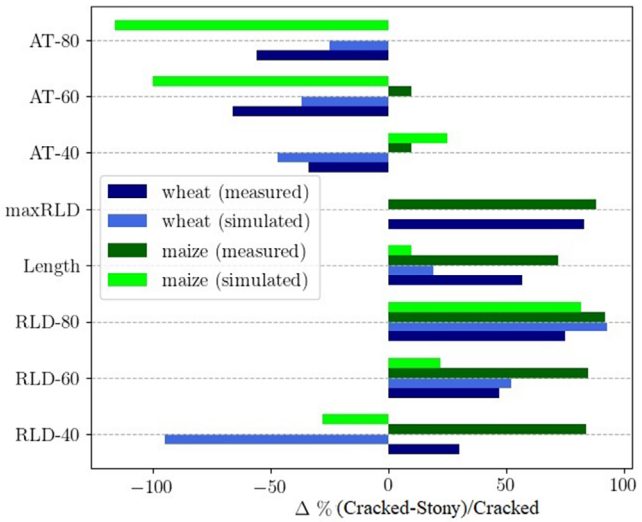

FIGURE 11 Comparison between measured and simulated differences in root system measures and between stony and cracked facilities for both wheat and maize (RLD = root length densities, length = total root length below 1 m^2 of soil surface up to 120-cm depth, maxRLD = depth at which maximum RLD is observed, and AT = median root arrival times at 40-, 60-, and 80-cm depths)

Although simulations also predict this trend for maize, except at 40-cm depth, observations for maize predict the opposite. However, there are of course substantially more roots in the cracked facility than in the stony facility. Simulation results and data also agree on the fact that the total root length below 1-m^2 surface area is larger in cracked facility than in stony facility. However, this is more pronounced in the observations than in the simulations. This could be due to the fact that observations also include differences in carbon availability, which is not included in the root architecture model. In heterogeneous soil conditions, root systems could respond by altering branching density, branching angle or root anatomy that could also cause changes in physiological behavior (Schwinning, 2010). However, anatomical changes that lead to changes in RLDs are also not considered in the model.

The depth at which the maximum RLD occurs is the same in the stony facility and the cracked facility according to simulations, whereas observations show that the depth at which the maximum RLD is found is much larger in the cracked facility than in the stony facility. This can be explained by the fact CPlantBox-simulated RLD profiles have a shape that decreases with depth (and thus the highest RLD is found in the top in both stony and cracked facilities), whereas observations show a greater RLD in deeper layers in the cracked facility.

4 | CONCLUSION

In this study, we presented a plot-scale root architecture growth model that explicitly considers stones as obstacles as well as cracks in soil. Root elongation was impeded by dynamically changing temperature and soil strength. Simulation studies of maize and wheat plants considering the combined effects qualitatively agreed with observation. We showed that simulated differences of characteristic root system measures between stony and cracked soils of otherwise same crop and weather conditions show similar trends as in the measurements obtained in the rhizotron facilities in Selhausen.

The simulation model enabled a deep analysis of the single processes that lead to the combined results. In a sensitivity analysis, we showed the strength of impact of stones and cracks to the plant rooting depth of maize and wheat. The presence of the stone fraction in soil significantly reduces the rooting depths due to tortuosity effect, which leads to accumulation of roots at shallower depths compared with homogeneous soil. Furthermore, we showed the dynamic impact of temperature and soil strength using RACs, showing strong dependence of the type of root architecture. Analyses of the single processes enable quantitative hypotheses for better experimental designs.

An important simplification of the model is that it only alters the root elongation rate. In heterogeneous soil conditions, root systems could respond by altering branching density or branching angle. Although these root system responses are already implemented in CPlantBox, the parameterization is challenging. Emerging approaches for parameterization of RSA of certain crops based on field sampling data are useful for understanding the alteration of parameters in heterogeneous growth mediums (Morandage et al., 2019). A further model limitation is the lack of shoot development and resulting carbon availability for root growth. Crop height and leaf area index for wheat and maize in both the stony facility and cracked facility are given in Supplemental Figure S9 as an indication of the differences in shoot development in two soils. Future work will require the extension of our approach to consider the whole plant so as to be able to predict the carbon availability for shoot and root growth.

ACKNOWLEDGMENTS

This work was supported by the Transregional Collaborative Research Centre 32 (TR32), which is funded by the Deutsche Forschungsgemeinschaft (DFG) and by the Deutsche Forschungsgemeinschaft (DFG, German Research Foundation) under Germany's Excellence Strategy—EXC 2070–390732324.

AUTHOR CONTRIBUTIONS

Shehan Morandage: Conceptualization; Data curation; Formal analysis; Investigation; Methodology; Software; Visualization; Writing-original draft; Writing-review & editing. Jan Vanderborght: Conceptualization; Formal analysis; Funding acquisition; Supervision; Writing-review & editing. Mirjam

Zörner: Methodology. Gaochao Cai: Methodology; Writing-review & editing. Daniel Leitner: Software; Visualization; Writing-original draft. Harry Vereecken: Funding acquisition; Supervision. Andrea Schnepf: Conceptualization; Formal analysis; Funding acquisition; Investigation; Methodology; Resources; Software; Supervision; Validation; Writing-review & editing.

CONFLICT OF INTEREST

The authors declare no conflict of interest.

ORCID

Shehan Morandage https://orcid.org/0000-0003-1309-7369
Jan Vanderborght https://orcid.org/0000-0001-7381-3211
Gaochao Cai https://orcid.org/0000-0003-4484-1146
Harry Vereecken https://orcid.org/0000-0002-8051-8517
Andrea Schnepf https://orcid.org/0000-0003-2203-4466

REFERENCES

Bengough, A. G. (1997). Modelling rooting depth and soil strength in a drying soil profile. *Journal of Theoretical Biology*, *186*, 327–338. https://doi.org/10.1006/jtbi.1996.0367

Bengough, A. G., Bransby, M. F., Hans, J., Mckenna, S. J., Roberts, T. J., & Valentine, T. A. (2006). Root responses to soil physical conditions; growth dynamics from field to cell. *Journal of Experimental Botany*, *57*, 437–447. https://doi.org/10.1093/jxb/erj003

Bengough, A. G., Croser, C., & Pritchard, J. (1997). A biophysical analysis of root growth under mechanical stress. *Plant and Soil*, *189*, 155–164. https://doi.org/10.1023/A:1004240706284

Bengough, A. G., Mckenzie, B. M., Hallett, P. D., & Valentine, T. A. (2011). Root elongation, water stress, and mechanical impedance: A review of limiting stresses and beneficial root tip traits. *Journal of Experimental Botany*, *62*, 59–68. https://doi.org/10.1093/jxb/erq350

Bizet, F., Bengough, A. G., Hummel, I., Bogeat-Triboulot, M. -. B., & Dupuy, L. X. (2016). 3D deformation field in growing plant roots reveals both mechanical and biological responses to axial mechanical forces. *Journal of Experimental Botany*, *67*, 5605–5614. https://doi.org/10.1093/jxb/erw320

Buczko, U., Kuchenbuch, R. O., & Gerke, H. H. (2008). Evaluation of a core sampling scheme to characterize root length density of maize. *Plant and Soil*, *316*, 205–215. https://doi.org/10.1007/s11104-008-9771-5

Cai, G., Morandage, S., Vanderborght, J., Schnepf, A., & Vereecken, H. (2018). Erratum to "Construction of minirhizotron facilities for investigating root zone processes" and "Parameterization of root water uptake models considering dynamic root distributions and water uptake compensation." *Vadose Zone Journal*, *17*, 170201. https://doi.org/10.2136/vzj2017.11.0201

Cai, G., Vanderborght, J., Couvreur, V., Mboh, C. M., & Vereecken, H. (2018). Parameterization of root water uptake models considering dynamic root distributions and water uptake compensation. *Vadose Zone Journal*, *17*, 160125. https://doi.org/10.2136/vzj2016.12.0125

Cai, G., Vanderborght, J., Klotzsche, A., Van Der Kruk, J., Neumann, J., Hermes, N., & Vereecken, H. (2016). Construction of minirhizotron facilities for investigating root zone processes. *Vadose Zone Journal*, *15*. https://doi.org/10.2136/vzj2016.05.0043

Clausnitzer, V., & Hopmans, J. W. (1994). Simultaneous modeling of transient three-dimensional root growth and soil water flow. *Plant and Soil*, *164*, 299–314. https://doi.org/10.1007/bf00010082

Colombi, T., Kirchgessner, N., Walter, A., & Keller, T. (2017). Root tip shape governs root elongation rate under increased soil strength. *Plant Physiology*, *174*, 2289–2301. https://doi.org/10.1104/pp.17.00357

Correa, J., Postma, J. A., Watt, M., & Wojciechowski, T. (2019). Soil compaction and the architectural plasticity of root systems. *Journal of Experimental Botany*, *70*, 6019–6034. https://doi.org/10.1093/jxb/erz383

de Moraes, M. T., Bengough, A. G., Debiasi, H., Franchini, J. C., Levien, R., Schnepf, A., & Leitner, D. (2018). Mechanistic framework to link root growth models with weather and soil physical properties, including example applications to soybean growth in Brazil. *Plant and Soil*, *428*, 67–92. https://doi.org/10.1007/s11104-018-3656-z

de Moraes, M. T., Debiasi, H., Franchini, J. C., Bonetti, J. D.e A., Levien, R., Schnepf, A., & Leitner, D. (2019). Mechanical and hydric stress effects on maize root system development at different soil compaction levels. *Frontiers in Plant Science*, *10*, 1358. https://doi.org/10.3389/fpls.2019.01358

Dexter, A. R. (1987). Mechanics of root growth. *Plant and Soil*, *98*, 303–312. https://doi.org/10.1007/BF02378351

Dexter, A. R., & Hewitt, J. S. (1978). The deflection of plant roots. *Journal of Agricultural Engineering Research*, *23*, 17–22. https://doi.org/10.1016/0021-8634(78)90075-6

Drennan, P. M., & Nobel, P. S. (1998). Root growth dependence on soil temperature for *Opuntia ficus-indica*: Influences of air temperature and a doubled CO_2 concentration. *Functional Ecology*, *12*, 959–964. https://doi.org/10.1046/j.1365-2435.1998.00276.x

Dunbabin, V. M., Postma, J. A., Schnepf, A., Pagès, L., Javaux, M., Wu, L., Leitner, D., Chen, Y. L., Rengel, Z., & Diggle, A. J. (2013). Modelling root-soil interactions using three-dimensional models of root growth, architecture and function. *Plant and Soil*, *372*, 93–124. https://doi.org/10.1007/s11104-013-1769-y

Eavis, B. W. (1972). Soil physical conditions affecting seedling root growth. *Plant and Soil*, *36*, 613–622. https://doi.org/10.1007/bf01373511

Ellis, B. A., & Kummerow, J. (1982). Temperature effect on growth rates of *Eriophorum vaginatum* roots. *Oecologia*, *54*, 136–137. https://doi.org/10.1007/BF00541120

Ephrath, J. E., Silberbush, M., & Berliner, P. R. (1999). Calibration of minirhizotron readings against root length density data obtained from soil cores. *Plant and Soil*, *209*, 201–208. https://doi.org/10.1023/A:1004556100253

Fakih, M., Delenne, J. Y., Radjai, F., & Fourcaud, T. (2017). Modeling root growth in granular soils: Effects of root stiffness and packing fraction. *EPJ Web of Conferences* 140, 14013. https://doi.org/10.1051/epjconf/201714014013

Falik, O., Reides, P., Gersani, M., & Novoplansky, A. (2005). Root navigation by self inhibition. *Plant Cell and Environment*, *28*, 562–569. https://doi.org/10.1111/j.1365-3040.2005.01304.x

Gao, Y., Duan, A., Qiu, X., Liu, Z., Sun, J., Zhang, J., & Wang, H. (2010). Distribution of roots and root length density in a maize/soybean strip intercropping system. *Agricultural Water Management*, *98*, 199–212. https://doi.org/10.1016/j.agwat.2010.08.021

Garré, S., Pagès, L., Laloy, E., Javaux, M., Vanderborght, J., & Vereecken, H. (2012). Parameterizing a dynamic architectural model

of the root system of spring barley from minirhizotron data. *Vadose Zone Journal*, *11*. https://doi.org/10.2136/vzj2011.0179

Grant, R. F. (1993). Simulation model of soil compaction and root growth. *Plant and Soil*, *150*, 15–24. https://doi.org/10.1007/BF00779171

Grismer, M. (1992). Cracks in irrigated clay soil may allow some drainage. *California Agriculture*, *46*, 9–11. https://doi.org/10.3733/ca.v046n05p9

Hlaváčiková, H., Novák, V., Kostka, Z., Danko, M., & Hlavčo, J., (2018). The influence of stony soil properties on water dynamics modeled by the HYDRUS model. *Journal of Hydrology and Hydromechanics*, *66*, 181–188. https://doi.org/10.1515/johh-2017-0052

Houlbrooke, D. J., Thom, E. R., Chapman, R., & Mclay, C. D. A. (1997). A study of the effects of soil bulk density on root and shoot growth of different ryegrass lines. *New Zealand Journal of Agricultural Research*, *40*, 429–435. https://doi.org/10.1080/00288233.1997.9513265

Huang, B. - R., Taylor, H. M., & McMichael, B. L. (1991). Growth and development of seminal and crown roots of wheat seedlings as affected by temperature. *Environmental and Experimental Botany*, *31*, 471–477. https://doi.org/10.1016/0098-8472(91)90046-Q

Hulugalle, N. R., Broughton, K. J., & Tan, D. K. Y. (2015). Root growth of irrigated summer crops in cotton-based farming systems sown in Vertosols of northern New South Wales. *Crop & Pasture Science*, *66*, 158–167. https://doi.org/10.1071/Cp14184

Jin, K., Shen, J., Ashton, R. W., Dodd, I. C., Parry, M. A. J., & Whalley, W. R. (2013). How do roots elongate in a structured soil? *Journal of Experimental Botany*, *64*, 4761–4777. https://doi.org/10.1093/jxb/ert286

Jin, W., Aufrecht, J., Patino-Ramirez, F., Cabral, H., Arson, C., & Retterer, S. T. (2020). Modeling root system growth around obstacles. *Scientific Reports*, *10*, 15868 https://doi.org/10.1038/s41598-020-72557-8

Kaspar, T. C., & Bland, W. L. (1992). Soil-temperature and root-growth. *Soil Science*, *154*, 290–299. https://doi.org/10.1097/00010694-199210000-00005

Kirby, J. M., & Bengough, A. G. (2002) Influence of soil strength on root growth: experiments and analysis using a critical-state model. *European Journal of Soil Science*, *53*, 119–127. https://doi.org/10.1046/j.1365-2389.2002.00429.x

Kolb, E., Legué, V., & Bogeat-Triboulot, M.-.B. (2017). Physical root-soil interactions. *Physical Biology*, *14*, 065004. https://doi.org/10.1088/1478-3975/aa90dd

Landl, M., Huber, K., Schnepf, A., Vanderborght, J., Javaux, M., Glyn Bengough, A., & Vereecken, H. (2017). A new model for root growth in soil with macropores. *Plant and Soil*, *415*, 99–116. https://doi.org/10.1007/s11104-016-3144-2

Landl, M., Schnepf, A., Uteau, D., Peth, S., Athmann, M., Kautz, T., Perkons, U., Vereecken, H., & Vanderborght, J. (2019). Modeling the impact of biopores on root growth and root water uptake. *Vadose Zone Journal*, *18*, 180196. https://doi.org/10.2136/vzj2018.11.0196

Macduff, J. H., Wild, A., Hopper, M. J., & Dhanoa, M. S. (1986). Effects of temperature on parameters of root-growth relevant to nutrient-uptake: Measurements on oilseed rape and barley grown in flowing nutrient solution. *Plant and Soil*, *94*, 321–332. https://doi.org/10.1007/Bf02374326

McMichael, B. L., & Quisenberry, J. E. (1993). The impact of the soil environment on the growth of root systems. *Environmental and Experimental Botany*, *33*, 53–61. https://doi.org/10.1016/0098-8472(93)90055-K

Mekonnen, K., Buresh, R. J., & Jama, B. (1997). Root and inorganic nitrogen distributions in sesbania fallow, natural fallow and maize fields. *Plant and Soil*, *188*, 319–327. https://doi.org/10.1023/A:1004264608576

Morandage, S., Schnepf, A., Leitner, D., Javaux, M., Vereecken, H., & Vanderborght, J. (2019). Parameter sensitivity analysis of a root system architecture model based on virtual field sampling. *Plant and Soil*, *438*, 101–126. https://doi.org/10.1007/s11104-019-03993-3

Nagel, K. A., Kastenholz, B., Jahnke, S., Van Dusschoten, D., Aach, T., Mühlich, M., Truhn, D., Scharr, H., Terjung, S., Walter, A., & Schurr, U. (2009). Temperature responses of roots: Impact on growth, root system architecture and implications for phenotyping. *Functional Plant Biology*, *36*, 947–959. https://doi.org/10.1071/Fp09184

Naseri, M., Iden, S. C., Richter, N., & Durner, W. (2019). Influence of stone content on soil hydraulic properties: Experimental investigation and test of existing model concepts. *Vadose Zone Journal*, *18*(1). https://doi.org/10.2136/vzj2018.08.0163

Onderdonk, J. J., & Ketcheson, J. W. (1973). Effect of soil temperature on direction of corn root growth. *Plant and Soil*, *39*, 177–186. https://doi.org/10.1007/Bf00018055

Osher, S., & Fedkiw, R. (2003). Signed distance functions. In S. Osher & R. Fedkiw (Eds.), *Level set methods and dynamic implicit surfaces*. Springer.

Pagès, L., Bruchou, C., & Garré, S. (2012). Links between root length density profiles and models of the root system architecture. *Vadose Zone Journal*, *11*. https://doi.org/10.2136/vzj2011.0152

Palta, J., M, L., & Irp, F. (2004). *Rooting patterns in wheat differing in vigour is related to the early uptake of nitrogen in deep sandy soils*. Paper presented at the 4th International Crop Science Congress, Brisbane, QLD, Australia. http://www.cropscience.org.au/icsc2004/poster/2/4/1/473_paltaja.htm

Pardo, A., Amato, M., & Chiarandà, F. Q. (2000). Relationships between soil structure, root distribution and water uptake of chickpea (*Cicer arietinum* L.). Plant growth and water distribution. *European Journal of Agronomy*, *13*, 39–45. https://doi.org/10.1016/S1161-0301(00)00056-3

Popova, L., Tonazzini, A., Russino, A., Sadeghi, A., & Mazzolai, B. (2013). Embodied behavior of plant roots in obstacle avoidance. In N. F. Lepora, A. Mura, H. G. Krapp, P. Verschure, & T. J. Prescott (Eds.), *Biomimetic and biohybrid systems* (pp. 431–433). Springer. https://doi.org/10.1007/978-3-642-39802-5_57

Popova, L., Van Dusschoten, D., Nagel, K. A., Fiorani, F., & Mazzolai, B. (2016). Plant root tortuosity: An indicator of root path formation in soil with different composition and density. *Annals of Botany*, *118*, 685–698. https://doi.org/10.1093/aob/mcw057

Porter, J. R., & Gawith, M. (1999). Temperatures and the growth and development of wheat: A review. *European Journal of Agronomy*, *10*, 23–36. https://doi.org/10.1016/S1161-0301(98)00047-1

Postic, F., Beauchêne, K., Gouache, D., & Doussan, C. (2019). Scanner-based minirhizotrons help to highlight relations between deep roots and yield in various wheat cultivars under combined water and nitrogen deficit conditions. *Agronomy*, *9*, 297. https://doi.org/10.3390/agronomy9060297

Postma, J. A., & Lynch, J. P. (2011). Root cortical aerenchyma enhances the growth of maize on soils with suboptimal availability of nitrogen, phosphorus, and potassium. *Plant Physiology*, *156*, 1190–1201. https://doi.org/10.1104/pp.111.175489

Postma, J. A., & Lynch, J. P. (2012). Complementarity in root architecture for nutrient uptake in ancient maize/bean and maize/bean/squash polycultures. *Annals of Botany*, *110*, 521–534. https://doi.org/10.1093/aob/mcs082

Postma, J. A., Kuppe, C., Owen, M. R., Mellor, N., Griffiths, M., Bennett, M. J., Lynch, J. P., & Watt, M. (2017). OpenSimRoot: Widening the scope and application of root architectural models. *New Phytologist*, *215*, 1274–1286. https://doi.org/10.1111/nph.14641

Richter, G. L., Monshausen, G. B., Krol, A., & Gilroy, S. (2009). Mechanical stimuli modulate lateral root organogenesis. *Plant Physiology*,*151*, 1855–1866. https://doi.org/10.1104/pp.109.142448

Sánchez, B., Rasmussen, A., & Porter, J. R. (2014). Temperatures and the growth and development of maize and rice: A review. *Global Change Biology*, *20*, 408–417. https://doi.org/10.1111/gcb.12389

Sattelmacher, B., Marschner, H., & Kühne, R. (1990). Effects of the temperature of the rooting zone on the growth and development of roots of potato (*Solanum tuberosum*). *Annals of Botany*, *65*, 27–36. https://doi.org/10.1093/oxfordjournals.aob.a087903

Schnepf, A., Leitner, D., Landl, M., Lobet, G., Mai, T. H., Morandage, S., Sheng, C., Zörner, M., Vanderborght, J., & Vereecken, H. (2018). CRootBox: A structural-functional modelling framework for root systems. *Annals of Botany*, *121*, 1033–1053. https://doi.org/10.1093/aob/mcx221

Schwinning, S. (2010). The ecohydrology of roots in rocks. *Ecohydrology*, *3*. 238–245. https://doi.org/10.1002/eco.134

Stadler, A., Rudolph, S., Kupisch, M., Langensiepen, M., Van Der Kruk, J., & Ewert, F. (2015). Quantifying the effects of soil variability on crop growth using apparent soil electrical conductivity measurements. *European Journal of Agronomy*, *64*, 8–20. https://doi.org/10.1016/j.eja.2014.12.004

Stendahl, J., Lundin, L., & Nilsson, T.: (2009). The stone and boulder content of Swedish forest soils. *Catena*, *77*, 285–291. https://doi.org/10.1016/j.catena.2009.02.011

Svane, S. F., Jensen, C. S., & Thorup-Kristensen, K. (2019). Construction of a large-scale semi-field facility to study genotypic differences in deep root growth and resources acquisition. *Plant Methods*, *15*, 26. https://doi.org/10.1186/s13007-019-0409-9

Tardieu, F. (1994). Growth and functioning of roots and of root systems subjected to soil compaction. Towards a system with multiple signalling? *Soil and Tillage Research*, *30*, 217–243. https://doi.org/10.1016/0167-1987(94)90006-x

Taylor, H. M., & Brar, G. S. (1991). Effect of soil compaction on root development. *Soil & Tillage Research*, *19*, 111–119. https://doi.org/10.1016/0167-1987(91)90080-H

Tracy, S. R., Black, C. R., Roberts, J. A., Sturrock, C., Mairhofer, S., Craigon, J., & Mooney, S. J. (2012). Quantifying the impact of soil compaction on root system architecture in tomato (*Solanum lycopersicum*) by X-ray micro-computed tomography. *Annals of Botany*, *110*, 511–519. https://doi.org/10.1093/aob/mcs031

Valentine, T. A., Hallett, P. D., Binnie, K., Young, M. W., Squire, G. R., Hawes, C., & Bengough, A. G. (2012). Soil strength and macropore volume limit root elongation rates in many UK agricultural soils. *Annals of Botany*, *110*, 259–270. https://doi.org/10.1093/aob/mcs118

Vansteenkiste, J., Van Loon, J., Garré, S., Pagès, L., Schrevens, E., & Diels, J. (2014). Estimating the parameters of a 3-D root distribution function from root observations with the trench profile method: Case study with simulated and field-observed root data. *Plant and Soil*, *375*, 75–88. https://doi.org/10.1007/s11104-013-1942-3

Vaz, C. M. P., Manieri, J. M., De Maria, I. C., & Th. Van Genuchten, M. (2013). Scaling the dependency of soil penetration resistance on water content and bulk density of different soils. *Soil Science Society of America Journal*, *77*, 1488–1495. https://doi.org/10.2136/sssaj2013.01.0016

Vincent, C. D., & Gregory, P. J. (1989). Effects of temperature on the development and growth of winter wheat roots. *Plant and Soil*, *119*, 87–97. https://doi.org/10.1007/bf02370272

Wasson, A. P., Rebetzke, G. J., Kirkegaard, J. A., Christopher, J., Richards, R. A., & Watt, M. (2014). Soil coring at multiple field environments can directly quantify variation in deep root traits to select wheat genotypes for breeding. *Journal of Experimental Botany*, *65*, 6231–6249. https://doi.org/10.1093/jxb/eru250

Weihermüller, L., Huisman, J. A., Lambot, S., Herbst, M., & Vereecken, H. (2007). Mapping the spatial variation of soil water content at the field scale with different ground penetrating radar techniques. *Journal of Hydrology*, *340*, 205–216. https://doi.org/10.1016/j.jhydrol.2007.04.013

White, C. A., Sylvester-Bradley, R., & Berry, P. M. (2015). Root length densities of UK wheat and oilseed rape crops with implications for water capture and yield. *Journal of Experimental Botany*, *66*, 2293–2303. https://doi.org/10.1093/jxb/erv077

Whiteley, G. M., & Dexter, A. R. (1984). Displacement of soil aggregates by elongating roots and emerging shoots of crop plants. *Plant and Soil*, *77*, 131–140. https://doi.org/10.1007/Bf02182917

Xu, C., Tao, H., Tian, B., Gao, Y., Ren, J., & Wang, P.u (2016). Limited-irrigation improves water use efficiency and soil reservoir capacity through regulating root and canopy growth of winter wheat. *Field Crops Research*, *196*, 268–275. https://doi.org/10.1016/j.fcr.2016.07.009

Zeng, G., Birchfield, S. T., & Wells, C. E. (2008). Automatic discrimination of fine roots in minirhizotron images. *New Phytologist*, *177*, 549–557. https://doi.org/10.1111/j.1469-8137.2007.02271.x

Zhan, A. I., & Lynch, J. P. (2015). Reduced frequency of lateral root branching improves N capture from low-N soils in maize. *Journal of Experimental Botany*, *66*, 2055–2065. https://doi.org/10.1093/jxb/erv007

Zhang, X., Chen, S., Sun, H., Wang, Y., & Shao, L. (2009). Root size, distribution and soil water depletion as affected by cultivars and environmental factors. *Field Crops Research*, *114*, 75–83. https://doi.org/10.1016/j.fcr.2009.07.006

Zhou, X. -. R., Schnepf, A., Vanderborght, J., Leitner, D., Lacointe, A., Vereecken, H., & Lobet, G., (2020). CPlantBox, a whole-plant modelling framework for the simulation of water- and carbon-related processes. *In Silico Plants*, *2*, diaa001, https://doi.org/10.1093/insilicoplants/diaa001

Zhuang, J., Yu, G. R., & Nakayama, K. (2001). Scaling of root length density of maize in the field profile. *Plant and Soil*, *235*, 135–142. https://doi.org/10.1023/A:1011972019617

Ziegler, C., Dyson, R. J., & Johnston, I. G. (2019). Model selection and parameter estimation for root architecture models using likelihood-free inference. *Journal of The Royal Society Interface*, *16*, 20190293. https://doi.org/10.1098/rsif.2019.0293

Zuo, Q., Shi, J., Li, Y., & Zhang, R. (2006). Root length density and water uptake distributions of winter wheat under sub-irrigation. *Plant and Soil*, *285*, 45–55. https://doi.org/10.1007/s11104-005-4827-2

SUPPORTING INFORMATION

Additional supporting information may be found online in the Supporting Information section at the end of the article.

How to cite this article: Morandage S, Vanderborght J, Zörner M, Cai G, Leitner D, Vereecken H. & Schnepf, A. Root architecture development in stony soils. *Vadose Zone J*. 2021;*20:*e20133. https://doi.org/10.1002/vzj2.20133